Journal of Engg. Research **Vol. 4 No. (3) September 2016** pp. 85-94

التحقق التجريبي من طريقة السلوك العكسي الايجابي الجديدة لاكتشاف شبكة عاكسة

شياو قيانج جو، هوايباو وانغ، يينغ زهانغ وجوشينج سان
قسم الهندسة الكهربائية، جامعة يانشان، الصين

الخلاصة

اكتشاف islanding هو واحدة من أهم القضايا لتطبيقات العاكس المتصلة بالشبكة. في هذه الورقة يتم تقديم طريقة جديدة لمكافحة islanding. تستخدم الطريقة تسلسل الجهد السلبي كمتغير ردود فعل إيجابية، وليس هناك حاجة إلى اضافة تسلسل اضطراب سلبي على الإطلاق. وبعد islanding، فإن رد الفعل الإيجابي يجبر العنصر ذو تسلسل الجهد السلبي بعيدا عن القيمة الاسمية. ويتم تقديم برنامج التسلسل السلبي لاكتشاف islanding بنجاح. وأخيرا، يتم تنفيذ الاختبارات التجريبية وذلك للتحقق من فعالية الطريقة المقترحة.

Experimental verification of a new positive feedback islanding detection method for grid-connected inverter

Xiaoqiang Guo, Huaibao Wang, Ying Zhang and Guocheng San

Department of Electrical Engineering, Yanshan University, China

**Corresponding Author: Email: Xiaoqiang Guo, gxq@ysu.edu.cn*

ABSTRACT

Islanding detection is one of the most important issues for grid-connected inverter applications. A new positive-feedback anti-islanding method is presented in this paper. It utilizes the negative sequence voltage component as a positive feedback variable, and no additional negative sequence disturbance is needed at all. After islanding, the positive feedback loop will force the negative sequence voltage component away from the nominal value. A new negative sequence estimation algorithm is also presented for the successful islanding detection. Finally, the experimental tests are carried out to verify the effectiveness of the proposed method.

Keywords: Grid-connected inverter; islanding detection; positive feedback.

INTRODUCTION

Islanding detection has a long history of research in literature, which may date back to the last century. The earlier investigations about islanding detection mainly focus on large-scale power networks (Goderya *et al*., 1980). Afterward, with the development of small-scale distributed renewable energy systems, the relevant research has shifted into photovoltaic grid-connected system applications during 1980s (Vachtsevanous & Kang, 1989). IEEE Std. 929-2000 specifies that a grid-connected inverter should cease to energize within 2s after islanding. Since islanding causes serious problems, such as threats to personnel safety, out-of-phase reclosing and degradation of power quality. Therefore, it is of great importance to achieve reliable islanding detection for grid-connected inverters (Guo *et al*., 2014).

Many islanding detection methods have been reported in the last decades. In general, they can be categorized into two groups: passive and active solutions (Yafaoui *et al*., 2012). Passive solutions are simple to implement, and detect the islanding by under/over frequency/voltage, total harmonic distortions, unbalanced factor, phase angle jump and rate of change of frequency. However, there is a potential risk of failure for anti-islanding protection; more specifically, nondetection zone (Ropp *et al*., 2000; Ye *et al*., 2004). In addition, some of these passive solutions have disadvantages of slow response and potential risk of false tripping.

On the other hand, the active solutions deliberately introduce a change or disturbance, and then monitor its response to confirm the islanding. The typical solutions include the power variation (Yu *et al*., 2008), active frequency drift (Yafaoui *et al*., 2012), current disturbance (Yu *et al*., 2012), sandia frequency shift (Wang *et al*., 2007), positive feedback (Wang *et al*., 2009), and so on. Among the active methods, positive feedback is an effective way for islanding detection. However, the conventional voltage/frequency positive feedback methods will force the PCC voltage to drift far away from the nominal value, which will be harmful for the seamless transfer of a grid-connected inverter to islanding operation for microgrid applications (Li *et al*., 2004; Guerrero *et al*., 2011).

Compared with the abovementioned methods, the contribution of this paper is to present a new positive-feedback anti-islanding method. The novelty and advantages of the proposed method are as follows.

(1) Do not cause any current harmonics, which is a common drawback in conventional anti-islanding methods such as the active frequency drift method.

(2) No additional periodical disturbances required.

(3) Islanding can be identified, even the amplitude and frequency of PCC voltage are still within the safe operating range, which is beneficial to the seamless transfer of a grid-connected inverter to islanding operation for micro-grid applications.

PROPOSED ISLANDING DETECTION METHOD

Figure 1 illustrates the schematic diagram of a grid-connected inverter, which operates in the current control mode (Guo *et al*., 2010). When the breaker *S* is closed, both the inverter and grid feed the local load. However, only the inverter energizes the load after the break *S* is open, due to network faults. It is so-called islanding, which should be detected in a reliable way.

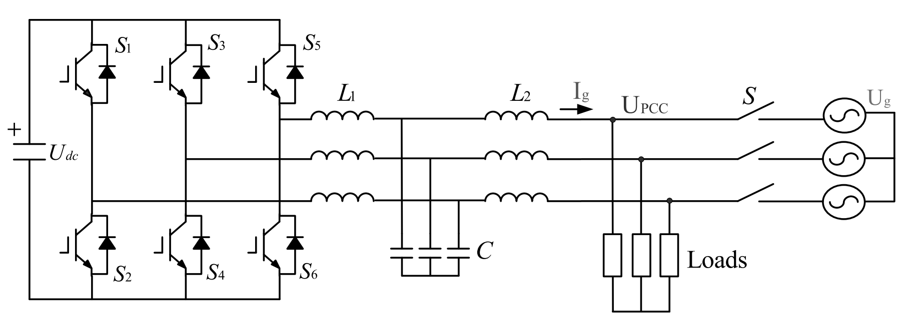

Fig. 1. Schematic diagram of the grid-connected inverter

The control model of grid-connectd inverter with the proposed islanding detection method is shown in Figure 2, where C(s) denotes the current controller, K is PWM gain. $U_{\alpha\beta}$ and $I_{\alpha\beta}$ are PCC voltage and grid current in $\alpha\beta$ stationary frame respectively. $F(U)$ is a function of negative sequence component of $U_{\alpha\beta}$. Note that the proposed islanding detection mehtod is enabled when S_n is closed, as shown in Figure 2 .

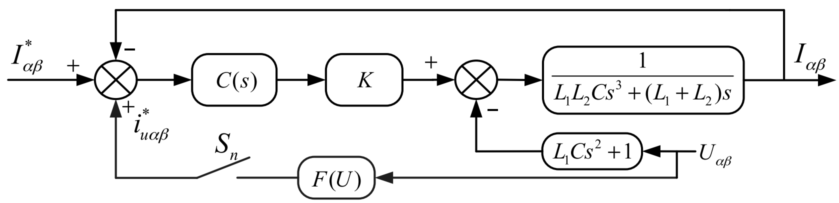

Fig. 2. Control model of grid-connected inverter with the islanidng detection fucntion

The initial grid current reference in stationary $\alpha\beta$ frame can be mathematically expressed as follows:

$$\begin{bmatrix} I^*_{\alpha} \\ I^*_{\beta} \end{bmatrix} = \begin{bmatrix} I_{\mathrm{m}}\sin(\omega t) \\ -I_{\mathrm{m}}\cos(\omega t) \end{bmatrix} \tag{1}$$

The function of F(U) is defined as:

$$\begin{bmatrix} I^*_{u\alpha} \\ I^*_{u\beta} \end{bmatrix} = F(U) = \begin{bmatrix} kU^-_{\mathrm{m}}\sin(\omega t) \\ kU^-_{\mathrm{m}}\cos(\omega t) \end{bmatrix} \tag{2}$$

Where U^-_{m} is the voltage amplitude of the negative sequence components at point of common coupling (PCC).

When the proposed islanding detection method is enabled, the current reference will be equal to $I^*_{u\alpha\beta}+I^*_{\alpha\beta}$, as shown in Figure 3. Assuming that the grid current $I_{\alpha\beta}$ can track its reference $I^*_{\alpha\beta}$ with zero steady-state error control, we can obtain the following equation.

$$\begin{bmatrix} I_{\alpha} \\ I_{\beta} \end{bmatrix} = \begin{bmatrix} I^*_{u\alpha}+I^*_{\alpha} \\ I^*_{u\beta}+I^*_{\beta} \end{bmatrix} = \begin{bmatrix} (kU^-_{\mathrm{m}}+I_{\mathrm{m}})\sin(\omega t) \\ (kU^-_{\mathrm{m}}-I_{\mathrm{m}})\cos(\omega t) \end{bmatrix} \tag{3}$$

Equation (3) can be rewritten in abc frame as follows:

$$\begin{bmatrix} I_{\mathrm{a}} \\ I_{\mathrm{b}} \\ I_{\mathrm{c}} \end{bmatrix} = \begin{bmatrix} I_{\mathrm{m}}\sin(\omega t)+kU^-_{\mathrm{m}}\sin(\omega t) \\ I_{\mathrm{m}}\sin(\omega t-120°)+kU^-_{\mathrm{m}}\sin(\omega t+120°) \\ I_{\mathrm{m}}\sin(\omega t+120°)+kU^-_{\mathrm{m}}\sin(\omega t-120°) \end{bmatrix} = \begin{bmatrix} (kU^-_{\mathrm{m}}+I_{\mathrm{m}})\sin(\omega t) \\ \sqrt{(kU^-_{\mathrm{m}})^2+I^2_{\mathrm{m}}-kU^-_{\mathrm{m}}I_{\mathrm{m}}}\,\sin(\omega t+\varphi_{\mathrm{b}}) \\ \sqrt{(kU^-_{\mathrm{m}})^2+I^2_{\mathrm{m}}-kU^-_{\mathrm{m}}I_{\mathrm{m}}}\,\sin(\omega t+\varphi_{\mathrm{c}}) \end{bmatrix} \tag{4}$$

Where $\tan\varphi_b = \dfrac{\sqrt{3}(I_m - kU_m^-)}{kU_m^- + I_m}$, $\tan\varphi_c = \dfrac{\sqrt{3}(kU_m^- - I_m)}{kU_m^- + I_m}$

From Equation (4), it can be observed that the proposed islanding detection method does not cause any current harmonics, which is a common drawback in conventional methods (Yafaoui *et al*., 2012).

$$\begin{bmatrix} U_a \\ U_b \\ U_c \end{bmatrix} = \begin{bmatrix} 311\sin(\omega t) \\ 311\sin(\omega t - 120°) \\ 311\sin(\omega t + 120°) \end{bmatrix} \tag{5}$$

Under normal grid conditions, the PCC voltage can be mathematically expressed as Equation (5). Note that there might be some harmonic components at PCC voltage, but in a very low level compared with fundamental compoeenents (Vannoy *et al*., 2007), so effect of the harmonic components can be neglected for simplicity.

When islanding occurs due to network faults, only the inverter energizes the load. The PCC voltage after islanding can be mathematically expressed as Equation (6).

$$\begin{bmatrix} U_a \\ U_b \\ U_c \end{bmatrix} = \begin{bmatrix} Z_a I_a \\ Z_b I_b \\ Z_c I_c \end{bmatrix} = \begin{bmatrix} |Z|(kU_m^- + I_m)\sin(\omega t + \varphi_z) \\ |Z|\sqrt{(kU_m^-)^2 + I_m^2 - kU_m^- I_m}\sin(\omega t + \varphi_b + \varphi_z) \\ |Z|\sqrt{(kU_m^-)^2 + I_m^2 - kU_m^- I_m}\sin(\omega t + \varphi_c + \varphi_z) \end{bmatrix} \tag{6}$$

where $Z(s) = \dfrac{1}{\frac{1}{R} + \frac{1}{Ls} + Cs} = \dfrac{RLs}{RLCs^2 + Ls + R}$ $|Z| = \dfrac{1}{\sqrt{(\frac{1}{R})^2 + (\omega C - \frac{1}{\omega L})^2}}$ $\angle\varphi_z = \text{atan}[\dfrac{R(1 - \omega^2 LC)}{\omega L}]$

Equation (6) indicates that negative sequence components (NSC) appear after islanding. Therefore, the NSC amplitude of PCC can be used as an indicator for islanding. In order to select the threshold value for islanding detection, the unbalanced factor is defined as U_m^+ / U_m^-, where U_m^+ and U_m^- are voltage amplitudes of the positive and negative sequence components, respectively.

In general, a small threshold of unbalanced factor leads to a fast islanding detection, but has a potential risk of nuisance false trip due to noises and disturbances. A large threshold of unbalanced factor results in a long time of islanding detection. Therefore, the threshold of unbalanced factor should be carefully selected. The specified unbalanced factor in IEC 61000-2-2 is less than 2% under normal conditions, while the specified unbalanced factor in IEEE Std-1159 is less than 3%. So the threshold of unbalanced factor should be greater than 3% for the indicator of islanding. In this paper, the threshold value is selected as 4%, which ensures the effective detection of islanding, and meanwhile avoids the false trip in case of small threshold.

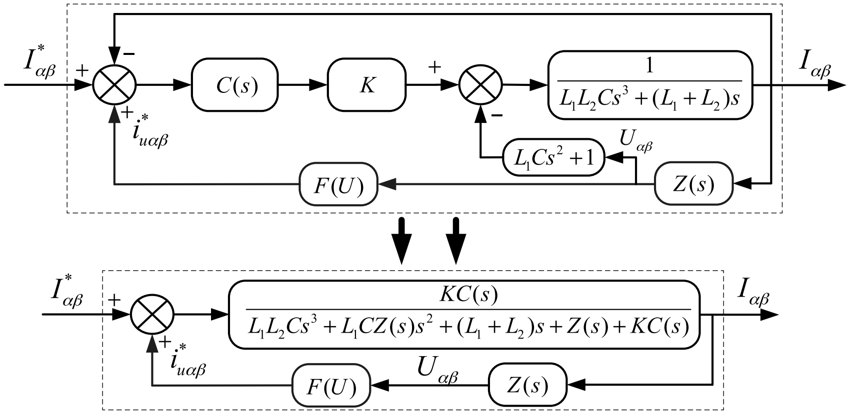

Fig. 3. System control model after islanding

Figure 3 illustrates the system control model after islanding. It can be observed that negative sequence components (NSC) will be amplified in a positive feedback manner. Therefore, the islanding can be easily detected. Note that the positive feedback gain has an effect on the real time detection of islanding. If the positive feedback gains are very low, the islanding will not be detected in a short timely way, to open the grid isolating circuit breaker. On the other hand, if the positive feedback gains are very large, the islanding can be detected fast. But, the voltage amplitude might be beyond the safe operating range, which affects the seamless transfer of grid-connected inverter to islanding operation for future micro-grid applications. Therefore, as for the positive feedback coefficient of F(U) (See Equation (2)) in Figure 3, it should be carefully designed to ensure the fast islanding detection, and meanwhile keep the amplitude and frequency of PCC voltage within the safe operating range (e.g. [(0.8, 1.1) pu and (f_0-0.7, f_0+0.5) Hz]). In this paper, the positive feedback coefficient is selected as k=0.01 pu.

Another consideration that should be noted is the effect of the penetration level of the DG units on the performance of the islanding detection method. In order to ensure the reliable islanding detection, all grid-connected inverters or DG units are generally designed with the same islanding method. In this way, the islanding can be successfully detected, because all inverters will respond in the same direction to force the negative sequence of PCC voltage, beyond the threshold value. On the other hand, for the high penetration level of the DG units with different islanding detection methods, it is more challenging and needs a systematic investigation, which is beyond the scope of this paper.

It should be noted that the behaviors of real DG units, such as PV panels, as well as the strong correlation between system disturbance and PV output voltage should be taken into account during the islanding events. In this case, the disturbances from

PV panel or PV output voltage will result in a transient response to trigger the positive feedback loop and the anti-islanding protection.

Note that the fast and accurate amplitude estimation of NSC is a necessity for the successful islanding detection. This paper introduces a new structure for NSC amplitude estimation, as depicted in Figure 4. It can achieve fast and accurate negative sequence extraction of $\hat{U}^{-}_{\alpha\beta 1}(s)$ even under a slight frequency variation. The NSC amplitude can be easily estimated as $U^{-}_{\mathrm{m}} = \sqrt{(\hat{U}^{-}_{\alpha})^2+(\hat{U}^{-}_{\beta})^2}$. Further details can be referred to (Guo *et al*., 2011).

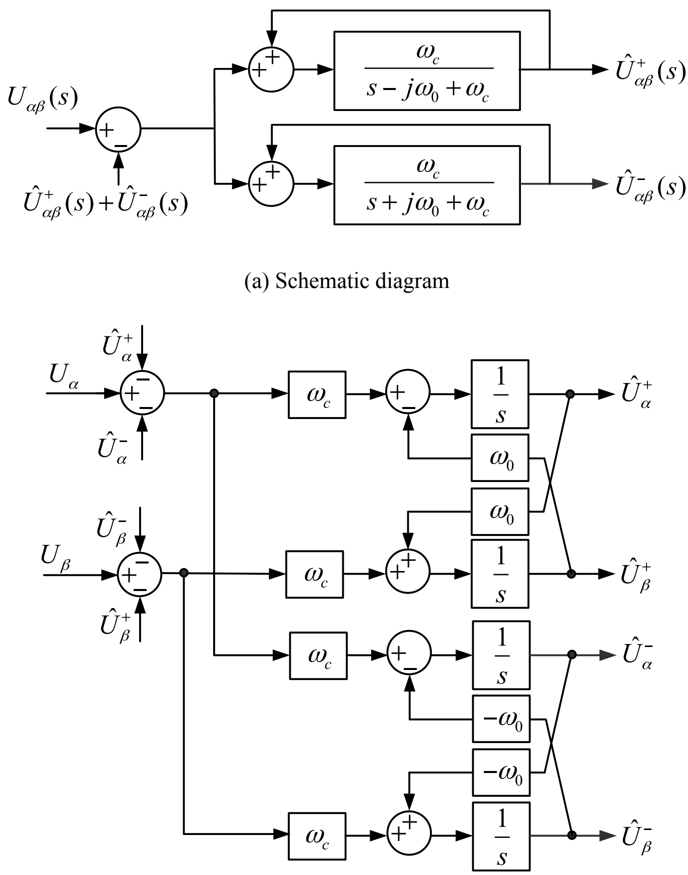

(a) Schematic diagram

(b) Implementation diagram

Fig. 4. Negative sequence estimation method

EXPERIMENTAL RESULTS

In order to verify the effectiveness of the proposed islanding detection method, the experimental tests are carried out on a grid-connected inverter with a LCL filter

(L_1= 3mH, L_2=1.5mH, C=9.4uF). The power level is 750VA in the experimental setup. The dc-link voltage of the inverter is fed with a DC power supply (rated 250V). The system output is connected to the grid through a Yy0 380/120-V 3-kVA three-phase transformer. The inverter is controlled by a 32-bit fixed-point 150MHz TMS320F2812 DSP. The switching is set to 10 kHz. The preset threshold value for the NSC amplitude is 0.04pu, and positive feedback coefficient *k*=0.01pu. The experimental results are shown as follows.

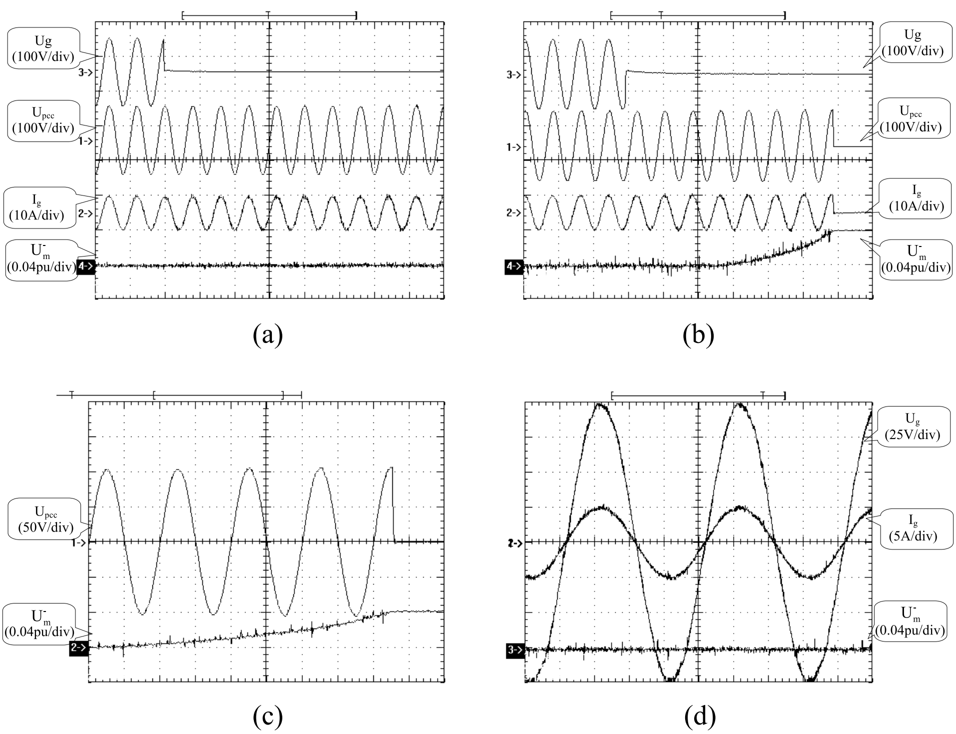

Fig. 5. Experimental results. (a) anti-islanding function is disabled after islanding. (b) anti-islanding function is enabled after islanding. (c) Zoom of (b). (d) anti-islanding function is enabled before islanding

Figure 5 (a) shows experimental result with the anti-islanding function disabled. It can be observed that PCC voltage remains unchanged before and after islanding, and the NSC amplitude keeps zero. It is mainly due to the power match between inverter and local load.

As shown in Fig. 5 (b), with the proposed anti-islanding function enabled, the NSC amplitude is amplified to trigger the anti-islanding protection, except for a slight unbalance factor of 4%. It is interesting that the amplitude and frequency of PCC voltage are still within the safe operating range [(0.8, 1.1) pu and (f_0-0.7, f_0+0.5) Hz], as specified in IEEE Std.929-2000. It is beneficial for the seamless transfer of a grid-connected inverter to islanding operation for micro-grid applications. Figure 5 (d) shows the experimental result with the proposed anti-islanding function enabled before islanding. It can be seen that the grid current is sinusoidal. In order to highlight the contribution of this paper, the obtained results have been compared with previously published method such as frequency deviations or THD of conventional method. Compared the widely used AFD methods (Yafaoui *et al*., 2012), where the frequency deviation is beyond 0.5Hz and THD is 5.16%, respectively. While for the proposed method, frequency deviation is less than 0.1Hz and THD is 1.83%, which verifies the effectiveness of the proposed method.

CONCLUSION

This paper has presented a new islanding detection method for the grid-connected inverter. With the proposed positive-feedback method, the islanding can be easily detected. In contrast to the existing methods, it can achieve the reliable islanding detection without deteriorating the grid current quality. Except for a slight unbalance factor of 4%, the amplitude and frequency of PCC voltage are still within the safe operating range, as specified in IEEE Std. 929- 2000. Therefore, it is attractive and promising for the micro-grid applications, where the seamless transfer to islanding operation is of great importance.

ACKNOWLEDGMENT

This work was supported by Science Foundation for Distinguished Young Scholars of Hebei Province (E2016203133) and China Postdoctoral Science Foundation (2015T80230).

REFERENCES

Goderya, F., Metwally, A. & Mansour, O. 1980. Fast detection and identification of islands in power networks. IEEE Trans. Power App. Syst., **99**(2):217–221.

Guerrero, J.M., Vasquez, J.C., Matas, J., Vicuna, L.G. & Castilla, M. 2011. Hierarchical control of droop-controlled AC and DC microgrids-A general approach toward standardization. IEEE Transactions on Industrial Electronics, **58**(1):158-172.

Guo, X., Lu, Z., Sun, X., Gu, H. & Wu, W. 2014. New grid impedance estimation technique for grid-connected power converters. Journal of Engineering Research, **2**(3):177-193.

Guo, X., Wu, W. & Chen, Z. 2011. Multiple-complex coefficient-filter based phase-locked loop and synchronization technique for three-phase grid-interfaced converters in distributed utility networks. IEEE Transactions on Industrial Electronics, 1194-1204.

Guo, X., Wu, W. & Gu, H. 2010. Modeling and simulation of direct output current control for LCL interfaced grid-connected inverters. Simulation Modelling Practice and Theory, 18:946–956.

Guo, X., Xu, D. &, Wu, B. 2014. Overview of anti-islanding US patents for grid-connected inverters. Renewable and Sustainable Energy Reviews, 40:311–317.

Li, Y., Vilathgamuwa, D. & Loh, P. 2004. Design, analysis and real-time testing of a controller for multibus microgrid system. IEEE Transactions on Power Electronics, **19**(5):1195–1204.

Ropp, M.E., Begovic, M. & Rohatgi, A. 2000. Determining the relative effectiveness of islanding prevention techniques using phase criteria and non-detection zones. IEEE Transactions on Energy Conversion, **15**(3):290–296.

Vachtsevanous, G. & Kang, H. 1989. Simulation studies of islanded behavior of grid connected photovoltaic systems. IEEE Transactions on Energy Conversion, **4**(2):177–183.

Vannoy, D.B., McGranaghan, M.F., Halpin, M., Moncrief, W.A. & Sabin, D. 2007. Roadmap for power-quality standards development. IEEE Transactions on Industry Applications, **43**(2):412–421.

Wang, X., Freitas, W., Xu, W. & Dinavahi, V. 2007. Impact of DG interface controls on the sandia frequency shift anti-islanding method. IEEE Transactions on Energy Conversions, **22**(3):792–794.

Wang, X., Freitas, W., Dinavahi, V. & Xu, W. 2009. Investigation of positive feedback anti-islanding control for multiple inverter-based distributed generators," IEEE Transactions on Power Systems, **24**(2):785–795.

Yafaoui, A., Wu, B. & Kouro, S. 2012. Improved active frequency drift anti-islanding detection method for grid connected photovoltaic systems. IEEE Transactions on Power Electronics, **27**(5):2367–2375.

Ye, Z., Kolwalker, A. Zhang,Y. Du, P. & Walling. R. 2004. Evaluation of anti-islanding schemes based on non-detection zone concept. IEEE Transactions on Power Electronics, **19**(5):1171–1176.

Yu, B., Matsui, M. & Yu G. 2011. A correlation-based islanding detection method using current-magnitude disturbance for PV system. IEEE Transactions on Industrial Electronics, **58**(7):2935–2943.

Yu, B., Matsui, M., So, H. & Yu G. 2008. A high power quality anti-islanding method using effective power variation. Solar Energy, **82**(4):368–378.

Submitted: 07/06/2015
Revised: 02/08/2015
Accepted: 06/12/2015